Dynamic viscoelasticity of end-linking α,ω-dimethyl silyl poly(propylene oxide) solutions near the gel point

Akihiro Koike, Norio Nemoto*, Masaoki Takahashi† and Kunihiro Osaki
Institute for Chemical Research, Kyoto University, Uji, Kyoto 611, Japan and
†Division of Material Chemistry, Kyoto University, Yoshida, Kyoto 606, Japan
(Received 10 November 1993)

Dynamic viscoelasticity of α,ω-dimethyl silyl poly(propylene oxide) solutions was studied through the gelation process with end-linking. The gel point was determined as the reaction time, $t=t_c$, at which the storage and the loss shear moduli, $G'(\omega)$ and $G''(\omega)$, respectively, both became proportional to ω^n over the whole ω range measured, where ω is the angular frequency and n is a constant. Effects of polymer molecular weight M and concentration c on the steady-state viscosity η before the gel point and the equilibrium modulus G_{eq} after the gel point were examined in terms of critical exponents, k and z, defined by power laws, $\eta \sim (|t-t_c|/t_c)^{-k} \sim \varepsilon^{-k}$ and $G_{eq} \sim \varepsilon^z$, respectively ($\varepsilon$ being the relative distance from the gel point). The three exponents n, k and z were found to take universal values of $n=0.66\pm0.02$, $k=1.0\pm0.1$ and $z=2.0\pm0.1$ irrespective of M and c for unentangled systems. In these systems, the reduced plot of $G_{eq}(\varepsilon)/G_\infty$ *versus* ε gave a single composite curve in the range of $0.1<\varepsilon<0.7$, where G_∞ was the modulus for the ideal network in which all functional groups reacted. The presence of entanglement coupling in the prepolymer solutions made the critical behaviour of η and G_{eq} obscure and affected the exponent values. The results were briefly compared with theoretical predictions.

(Keywords: dynamic viscoelasticity; end-linking polymer; gelation)

INTRODUCTION

Winter and his coworkers[1,2] postulated that the gel point could be accurately determined as the point where both the storage and the loss moduli, $G'(\omega)$ and $G''(\omega)$, respectively, were proportional to a power of the angular frequency, ω^n, over the wide range of angular frequency experimentally accessible. Since then, dynamic viscoelasticity[3-17] along with scattering methods[18-27] has been widely used for studies of the critical behaviour of various gelling systems. Viscoelastic measurements provide, in principle, three exponents; one exponent, n, appears in equation (1) being valid at the gel point:

$$G'(\omega) \sim G''(\omega) \sim \omega^n \quad (1)$$

k and z, appearing in equations (2) and (3), respectively, express divergence of the steady-state viscosity η and growth of the equilibrium modulus G_{eq} in the critical region before and after the gel point, respectively:

$$\eta \sim \varepsilon^{-k} \quad (2)$$

$$G_{eq} \sim \varepsilon^z \quad (3)$$

Here ε is the relative distance from the gel point ($\varepsilon=|p-p_c|/p_c$, where p is an extent of reaction in the gelation process and p_c is the value at the gel point). Experimental results of n, k and z have been compared with the prediction of classical theory[28,29] and those of modern theories developed on the basis of the self-similar structure of the critical gel[30-39].

These experimental results indicate that n is not constant but takes values in the range of $0<n<1$, depending on the species of gelling materials, a stoichiometric ratio, the gel preparation method and also on polymer molecular weight and concentration. Accordingly, it is not surprising even if neither k nor z take the universal value. This non-universality thus makes it impossible to judge what theory correctly predicts the critical behaviour near the sol–gel transition and resulting gel structure.

From an experimental point of view, the non-universality may be partly ascribed to the effect of entanglements on the branched structure formed in the gelation process, which is entirely neglected in the theoretical treatment owing to mathematical complexity. Indeed Izuka *et al.*[9] observed that the exponent n decreased with increasing molecular weight of prepolymers. Since the entanglement effect on the dynamics of linear flexible polymers is clearly manifested in the dramatic change in the concentration dependence of η with dilution, it is worthwhile to study how dilution affects the critical behaviour. There have only been fragmented reports[8,16] examining the effect of dilution so far.

In this paper, effects of polymer molecular weight M and concentration c on the gelation process are studied from dynamic viscoelastic measurements on α,ω-dimethyl silyl poly(propylene oxide) solutions at the balanced stoichiometric condition. The results show that the three exponents take universal values for unentangled solutions

* To whom correspondence should be addressed. Permanent address: Department of Applied Science, Kyushu University, 6-10-1 Hakozaki, Fukuoka 812, Japan

0032-3861/94/14/3005–06
© 1994 Butterworth-Heinemann Ltd

independent of M and c, while the entanglements not only affect the values of the three exponents but also make the critical behaviour obscure.

EXPERIMENTAL

Materials

The prepolymer sample used in this study is linear poly(propylene oxide) with dimethoxy silyl groups at both chain ends (PPO-Si). We used two samples of different molecular weight. The number-average molecular weight, M_n, and the ratio of the weight- to the number-average molecular weight, M_w/M_n, of the sample designated as MS20A are 7500 and 2.1, respectively, and those of SAT-L are 2000 and 1.3. These samples and the reaction catalyst (no. 918), which is a mixture including dibutyltin oxide as a major component, were supplied by Kaneka Corporation. *Figure 1* illustrates the reaction scheme for the network formation by end-linking. Hydrolysis of dimethoxy silyl groups is followed by the formation of the siloxane bonds between neighbouring polymers, which finally leads to a three-dimensional network.

The n-butyl acetate was used as a diluting agent, because it dissolves in both PPO-Si and water and has a relatively high boiling point (126°C). The solutions were prepared by mixing prescribed amounts of PPO-Si and n-butyl acetate. Then distilled water (equal number of moles to that of the functional group) and the catalyst (3 wt% PPO-Si) were added. The weight fractions of the polymer were 0.96, 0.82, 0.73, 0.59, 0.49, 0.39, 0.33 and 0.25 for MS20A solutions and 0.94, 0.72, 0.48 and 0.25 for SAT-L solutions. The solutions were stirred for ~15 min, and transferred into the rheometer at 25.0±0.1°C.

Method

We used a stress-controlled rheometer (Carri-MED CSL-100) with a 6 cm parallel-plate configuration, and measured dynamic storage and loss shear moduli, G' and G'', in the ω range from 0.1 to 100 rad s^{-1} at 25.0±0.1°C. In the critical region before the gel point, η was also measured at low shear rates, and in the critical region after the gel point creep measurements were conducted to estimate equilibrium compliance J_e, which is equal to the inverse of G_{eq}.

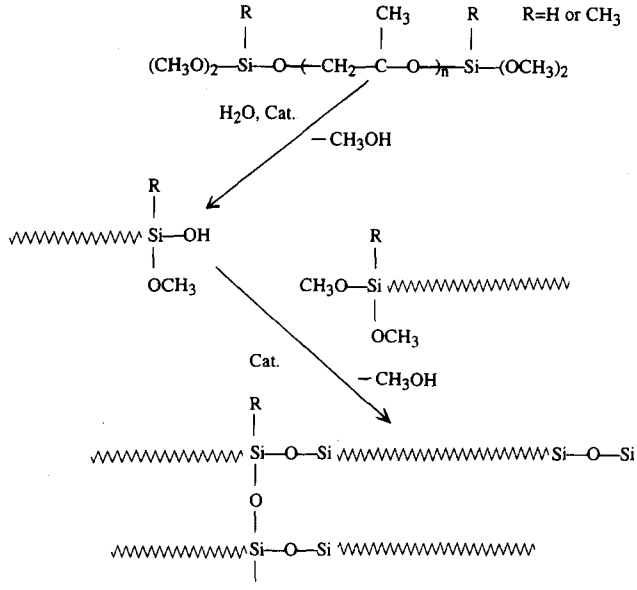

Figure 1 Reaction scheme of PPO-Si in the gelation process

RESULTS AND DISCUSSION

Steady flow property of prepolymer

Figure 2 shows a double logarithmic plot of steady-state viscosity before the crosslinking reaction, $\eta_{t=0}$, of MS20A and SAT-L solutions *versus* polymer weight fraction w_f. For the MS20A system, the slope changed from 3.0 for $w_f<0.63$ to 9.9 for $w_f>0.63$. On the other hand, $\eta_{t=0}$ of the SAT-L system gradually increased with w_f and the slope was ~3.1. The ω dependence of the SAT-L sample in the melt shows that chains are not entangled[40]. The entanglement molecular weight, $M_{e,0}$, of poly(propylene oxide) in bulk is estimated as 2900[41]. The slope of the MS20A (3.0) is nearly equal to that of SAT-L (3.1), which may indicate that the MS20A chains are not entangled below $w_f^*(=0.63)$, but are entangled above w_f^*.

Determination of the gel point

At the gel point G' and G'' are both proportional to ω^n, as stated in the Introduction. *Figure 3* shows a double logarithmic plot of G' and G'' *versus* ω for the MS20A system at five w_f values (0.96, 0.73, 0.59, 0.39, 0.25) at the gel point. Values of n and the critical (gelation) time, t_c, may be obtained from this figure. Because of uncertainties in such estimates, however, we determined n and t_c as

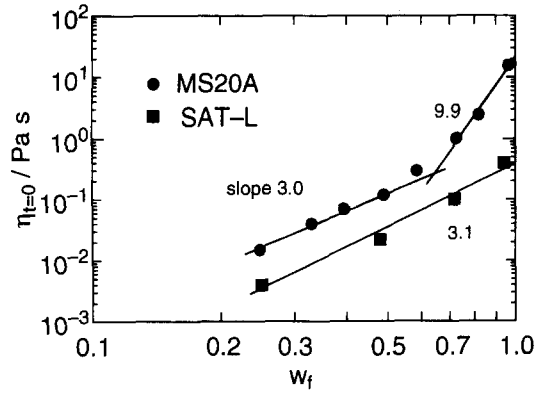

Figure 2 Double logarithmic plot of the viscosity before reaction, $\eta_{t=0}$, *versus* weight fraction, w_f, for MS20A and SAT-L solutions

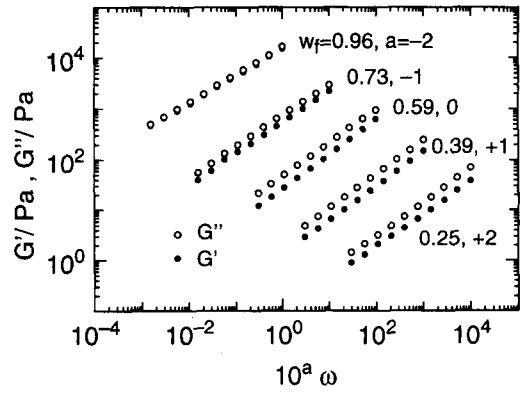

Figure 3 Angular frequency dependence of $G'(\omega)$ and $G''(\omega)$ of five MS20A solutions with w_f from 0.25 to 0.96 at the gel point. The data are shifted to avoid overlapping of data points by 10^a as indicated in the figure

follows. When G' and G'' are both proportional to ω^n over a wide ω range, $\tan\delta(=G''/G')$ is equal to $\tan(n\pi/2)$ from the Kramer–Kronig relationship[4]. This indicates that $\tan\delta$ must be independent of ω at the gel point. *Figure 4* shows the time dependence of $\tan\delta$ for the MS20A solution with $w_f=0.39$ at four different ω values (100, 14.4, 2.07, 0.30 rad s^{-1}). The four curves meet at one point in the measured ω range. This plot provides a more accurate determination of the gel point as the crossing point and accordingly of n and t_c at all w_f.

The time dependence of $\tan\delta$ in *Figure 4* suggests that viscoelastic properties of the system in the gelation process can be separately discussed by dividing them into three regions: region 1, where $\tan\delta$ gradually increases with reaction time t and reaches a maximum; region 2, where $\tan\delta$ after the maximum decreases with t, rapidly at higher ω to the gel point; and region 3, beyond the gel point. In region 1, all the solutions including the melt were essentially viscous Newtonian fluids so that the behaviour of $G'\sim\omega^2$ and $G''\sim\omega^1$ were clearly observed, and η gradually increased with t. In region 2, the solutions were no longer viscous fluids. The η increased very rapidly compared to region 1, in accordance with the decrease in $\tan\delta$ (the solutions became more and more elastic, and G' increased more rapidly than G''). The critical region is included in this region. In region 3, all the samples behaved elastically. The value of G_{eq} became larger and larger with reaction time, indicating further development of a three-dimensional network structure.

At the gel point

Table 1 gives experimental results on the exponent n at the gel point and t_c for all solutions. *Figure 5* shows the weight fraction dependence of n. For the MS20A system, n takes the smallest value of 0.51 at $w_f=0.96$, increases with decreasing w_f and then levels off below $w_f=0.50$, where $n=0.66\pm0.02$. On the other hand, n for SAT-L is independent of w_f at all concentrations measured, and equal to the constant value of $n=0.66\pm0.02$ obtained for the MS20A solutions with $w_f<0.50$.

In referring to the viscosity behaviour of the prepolymer solutions, these results clearly demonstrate that the polymer fractal structure at the gel point is affected by the presence of entanglement coupling in the prepolymer

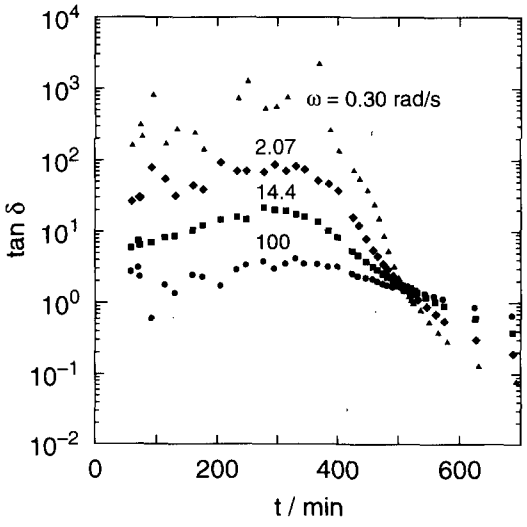

Figure 4 Time evolution of $\tan\delta$ for the MS20A ($w_f=0.39$) solution at four angular frequencies

Table 1 Experimental results at the gel point

MS20A					SAT-L				
W_f	n	t_c (min)	S^a	S^b	W_f	n	t_c (min)	S^a	S^b
0.96	0.51	213	1200	3200	0.94	0.67	120	49	54
0.82	0.57	211	250	490	–	–	–	–	–
0.73	0.59	216	120	200	0.72	0.68	145	14	17
0.59	0.63	295	22	48	–	–	–	–	–
0.49	0.66	357	11	14	0.48	0.68	223	2.5	6.8
0.39	0.67	525	4.8	8.0	–	–	–	–	–
0.33	0.68	680	2.5	4.4	–	–	–	–	–
0.25	0.67	1031	1.5	2.4	0.25	0.66	585	0.5	1.3

[a] $S=G'(\omega)/\omega^n\Gamma(1-n)\cos\delta$
[b] $S=G_\infty(\eta_{t=0}/G_\infty)^n$

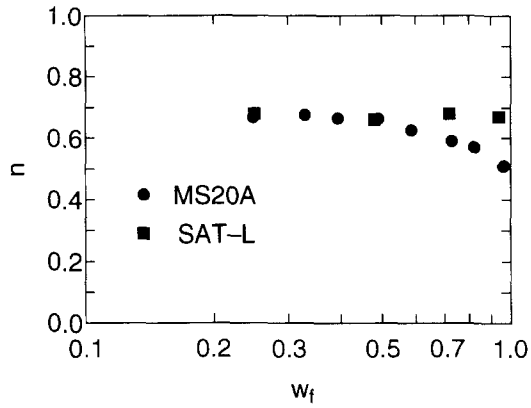

Figure 5 Dependence of n on weight fraction

solution. We find that n takes the universal value of 0.66, independent of polymer concentration and molecular weight for the unentangled solutions. Entanglements also seem to affect the value of t_c to some extent. The gelation is appreciably prolonged by dilution for unentangled solutions, whereas such an increase in t_c with dilution is suppressed by entanglements as is found for the MS20A solutions of $w_f\geqslant0.73$ (*Table1*).

Recently Izuka *et al.*[9] have shown that the gel strength S, characteristic of viscoelasticity at the gel point and defined by equation (4), is directly related to G_e of the fully crosslinked polymer and the viscosity $\eta_{t=0}$ of the prepolymer:

$$G'(\omega)=S\omega^n\Gamma(1-n)\cos\delta \qquad \text{at } t=t_c \tag{4}$$

$$S=G_e(\eta_{t=0}/G_e)^n \tag{5}$$

The value of S is easily estimated from $G'(\omega)$ data at $t=t_c$ by equation (4) and may be compared with the corresponding value calculated from equation (5) when $\eta_{t=0}$ and G_e are known. We have $\eta_{t=0}$ data of the prepolymer solutions, but we observed that a gradual but continuous increase in G_{eq} persisted for our system in the region of $t\gg t_c$ as the chemical reaction proceeded. Therefore G_e was here estimated as $G_e=G_\infty=cRT/M_n$ for the unentangled solutions, and as $G_\infty=c^2RT/M_{e,0}$ for the entangled MS20A solutions, assuming that all entanglement coupling points were entrapped in the critical gel and effectively acted as crosslinks. The G_∞ is the modulus of the fully crosslinked system. The true G_e value is surely smaller than G_∞, since a fraction of functional groups remains unreacted even at $t\to\infty$. The results are listed

in *Table 1*. The S value from equation (5) is always larger than that from equation (4) and may be ascribed to an overestimate of G_e as $G_e = G_\infty$. However the ratio is close to unity for some solutions and at most 3 for other solutions, in spite of a large change in S with molecular weight and concentration by nearly four orders of magnitude. It is to be noted that entanglements affect both $\eta_{t=0}$ and G_{eq} ($=G_\infty$). Thus we may be allowed to make such a conjecture that the structure of the critical gel is controlled by the molecular weight and the concentration of the prepolymer solution.

Before the gel point

In region 1 far from the gel point, all the samples behaved as viscous fluids. Therefore we measured η as a function of reaction time t by both oscillatory and steady flow measurements. In the first stage of the reaction (region 1), complex viscosity $|\eta^*|$ was found to be independent of ω and equal to η obtained from the flow measurement. As the reaction time approached t_c (region 2), $|\eta^*|$ became dependent on ω (shear thinning occurred at higher frequency). With $t/t_c < 0.70$, the value of $|\eta^*|$ at the low frequency end ($\omega \sim 0.1$ rad s^{-1}) remained nearly constant and was in good agreement with η. Near the gel point, we attempted to obtain the value of η at t (shear rate ~ 0.1 s^{-1}) as close to the gel point as possible by the flow measurement.

Figure 6 shows the time dependence of η for the MS20A solutions at eight concentrations, where the ordinate is reduced by $\eta_{t=0}$, and the abscissa by t_c. For the unentangled MS20A solutions at lower w_f, $\eta/\eta_{t=0}$ first increased very slowly, and then showed rapid increase at around $t/t_c = 0.80$. On the other hand, at higher w_f, $\eta/\eta_{t=0}$ of the entangled solutions started to increase at $t/t_c \ll 0.80$. *Figure 4* shows the time dependence of $\tan\delta$ for the MS20A solution with $w_f = 0.39$ at four angular frequencies. Before the gel point, $\tan\delta$ had a maximum value and then decreased. It was found that, in all the cases where entanglements were absent in the solution, the time (t/t_c) when $\tan\delta$ had the maximum value was in good agreement with the time when η started to increase rapidly.

We could not directly measure an extent of reaction p. Here we simply assume[16] that ε is represented by $\varepsilon = |t - t_c|/t_c$. The η values of the MS20A and SAT-L solutions are plotted against ε in *Figures 7* and *8*, respectively. Following the scaling theory which predicts the power law of $\eta \sim \varepsilon^{-k}$ before the gel point, we fitted the η data in the critical region (region 2) with a straight line from which k was obtained as a slope. The results are summarized in *Table 2*. Values of k for the MS20A solutions with $w_f < w_f^* = 0.63$ are almost constant (1.0 ± 0.1) and this value is also obtained for the SAT-L solutions over the whole range of w_f. For the entangled MS20A solutions with $w_f > 0.63$, k increased with increasing concentration. As is found for the exponent n, the exponent k for η takes a universal value of 1.0 ± 0.1 as far as the prepolymers are unentangled.

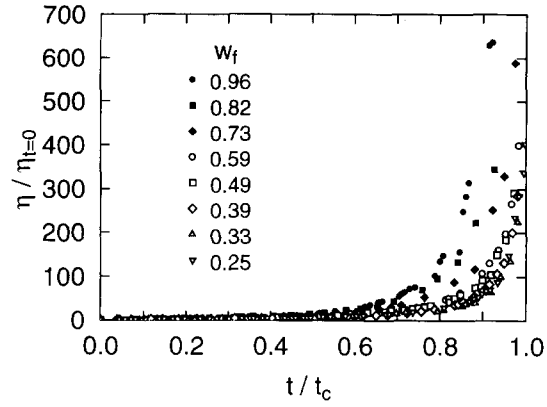

Figure 6 Time evolution of viscosity η divided by $\eta_{t=0}$ for MS20A solutions

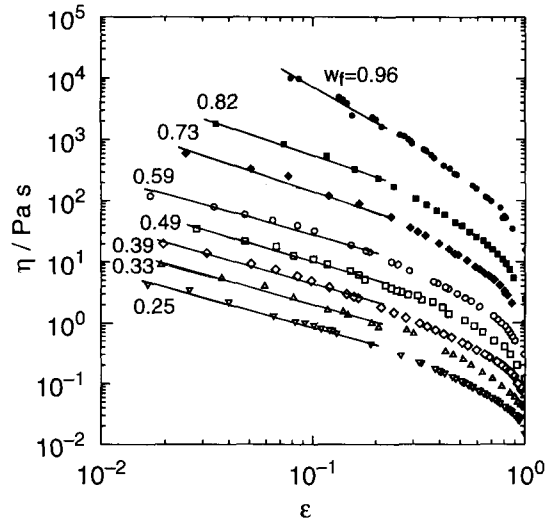

Figure 7 Double logarithmic plot of viscosity η *versus* ε for MS20A solutions. Here ε is a relative distance from the gel point defined as $\varepsilon \equiv |t - t_c|/t_c$. Straight lines are drawn following the scaling theory which predicts $\eta \sim \varepsilon^{-k}$ in the critical region

Table 2 Values of the two exponents k and z and calculated values of n and d_f

MS20A					SAT-L				
w_f	k	z	n	d_f	w_f	k	z	n	d_f
0.96	1.9±0.1	1.5±0.1	0.43	1.98	0.94	1.0±0.1	2.0±0.1	0.67	1.78
0.82	1.3±0.1	1.6±0.1	0.54	1.91	–	–	–	–	–
0.73	1.2±0.1	1.7±0.1	0.59	1.89	0.72	1.1±0.1	2.0±0.1	0.66	1.77
0.59	1.0±0.1	1.9±0.1	0.65	1.84	–	–	–	–	–
0.49	1.0±0.1	1.9±0.1	0.64	1.79	0.48	1.1±0.1	2.1±0.1	0.66	1.79
0.39	1.0±0.1	1.9±0.1	0.64	1.78	–	–	–	–	–
0.33	1.0±0.1	1.9±0.1	0.64	1.77	–	–	–	–	–
0.25	1.0±0.1	1.9±0.1	0.65	1.78	0.25	1.0±0.1	2.0±0.1	0.67	1.77

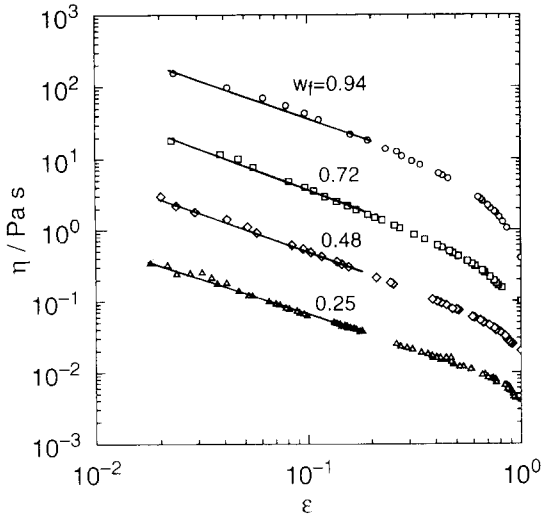

Figure 8 Double logarithmic plot of viscosity η *versus* ε for SAT-L solutions. Values of k are obtained as a slope of straight lines fitted to respective solution data

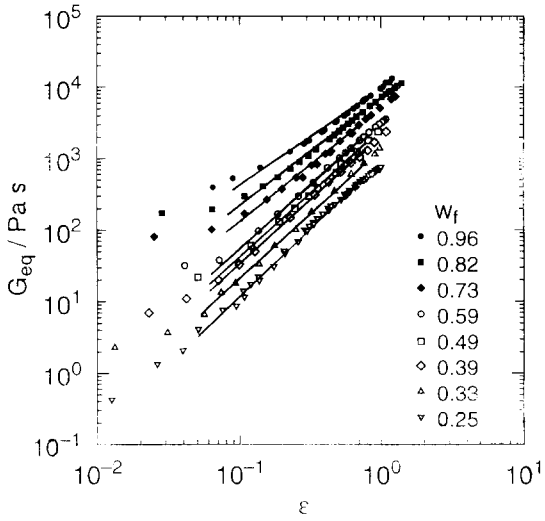

Figure 9 Double logarithmic plot of equilibrium modulus G_{eq} *versus* ε for MS20A solutions. Straight lines are drawn following the scaling theory which predicts $G_{eq} \sim \varepsilon^z$ in the critical region

After the gel point

Beyond the gel point, the largest cluster is fully developed from one side to the other side of the sample volume, so that the system may be characterized by G_{eq} to be estimated as the plateau value at the low ω end in the $G'(\omega)$ *versus* ω plot. The ε dependence of G_{eq} is shown in *Figures 9* and *10* for the MS20A and the SAT-L solutions, respectively. As the concentration increased, G_{eq} became larger at the same ε in both figures as expected. The G_{eq} could be accurately measured at small ε very close to the gel point at lower concentrations because t_c was longer at lower concentration. The scaling theory predicts that G_{eq} is proportional to ε^z in the critical region [equation (3)]. Surprisingly, the data of the unentangled systems were found to be located on straight lines in the very wide range of ε from 0.08 to 0.70. Values of z thus determined are listed in *Table 2*. In the case where entanglement coupling is not present for the prepolymer solutions, i.e. for the MS20A solutions with $w_f < 0.63$ and all SAT-L solutions, z is independent of concentration and may have very weak molecular weight dependence. The average of the MS20A solutions (1.9 ± 0.1) is just a little smaller than the corresponding value (2.0 ± 0.1) of the SAT-L solutions. In taking into account the experimental uncertainty of 0.1 involved in the estimate of z, however, it should be noted that z is hardly dependent on the molecular weight of the prepolymer. On the other hand, the behaviour of G_{eq} for the MS20A solutions with $w_f \geqslant 0.75$ is different from the unentangled system. Here G_{eq} seems to change its slope in *Figure 9* gradually and continuously with ε, and the power law may not be applicable for those solutions in a strict sense. When the forced fit by a straight line is made to the data points in the range of $0.10 \leqslant \varepsilon < 0.70$, we obtain z given in *Table 2*, which is appreciably smaller than the constant value at lower w_f and seems to decrease with increasing w_f.

In the preceding section, we argued that the structure of the critical gel was controlled by the molecular weight and the concentration of the prepolymer solution. By extending this conjecture to the time evolution of the gel structure after the gel point, we examined a possibility that the reduced plot of the $G_{eq}(\varepsilon)/G_\infty$ *versus* ε might give a single master curve for all solutions. As *Figure 11* shows, the reduced equilibrium moduli data of the unentangled solution form one composite curve in the region of $0.1 < \varepsilon < 0.7$. Furthermore, the reduced moduli data of the entangled MS20A solutions ($w_f = 0.96$, 0.82 and 0.73) are also closely located on the master curve for $0.2 < \varepsilon < 0.8$. Entanglement coupling present in the prepolymer solution should be considered to have been trapped during end-crosslinking and to act as if they were true crosslinks in the system. This idea is consistent with the idea that all G_{eq} data of entangled solutions in the small ε region deviate upward from the master curve and the deviation becomes larger with increasing concentration (the number of entanglements). The above results once again emphasize the importance of molecular weight and concentration of the prepolymer solution for the gelation process.

Comparison with theory

Our viscoelastic study on the gelation process of the PPO-Si solutions by end-linking has revealed that the critical behaviour of the unentangled solution is well represented by the universal values of $n = 0.66 \pm 0.02$, $k = 1.0 \pm 0.1$ and $z = 2.0 \pm 0.1$. The scaling theory[11,13]

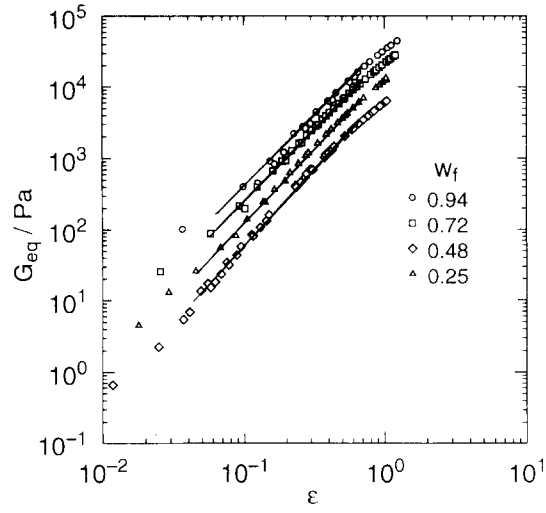

Figure 10 Double logarithmic plot of equilibrium modulus G_{eq} *versus* ε for SAT-L solutions. Values of z are obtained from straight lines fitted to the respective solution data

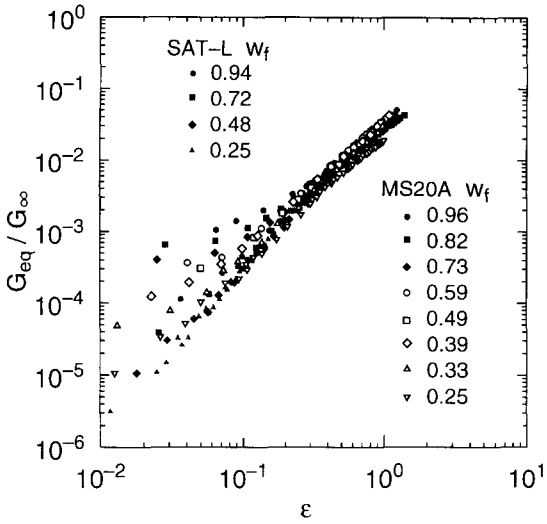

Figure 11 Double logarithmic plot of the reduced equilibrium modulus G_{eq}/G_∞ *versus* ε for MS20A and SAT-L solutions. The master curve is obtained for unentangled solutions, independent of molecular weight and concentration

interrelates the three exponents by equation (6):

$$n = z/(k+z) \tag{6}$$

Values of n were calculated for all solutions by equation (6) and are summarized in *Table 2* for comparison with the experimental values given in *Table 1*. Excellent agreement is obtained for both the MS20A and SAT-L solutions except the MS20A solution with $w_f = 0.96$, in which the experimental value is larger than the calculated one.

The percolation theory[35] predicts:

$$n_p = d/(d_f+2) \tag{7}$$

where d is the spatial dimension and d_f is the fractal dimension which relates the molecular weight of branched polymer to its spatial size R by $R^{d_f} \sim M$. The n_p takes 2/3 in the case that the excluded volume effect is fully taken into account to the conformation of large clusters in the critical region. This value apparently agrees with the universal value of $n = 0.66$ obtained over the wide range of polymer concentration. It is well known that the excluded volume effect is screened out in the concentrated solution as well as in bulk. Therefore the chain conformation of SAT-L at higher w_f should be the unperturbed one. Thus the agreement between theory and experiment seems only fortuitous. The computer simulation[14] on the basis of the percolation theory gives $k_p = 1.33$ and $z_p = 2.67$, respectively. These values are appreciably larger than the universal values of $k = 1.0$ and $z = 2.0$ obtained for the unentangled solutions. The simulated values also differ from those for the entangled solutions. This again discloses the shortcoming of the percolation theory.

Muthukumar[34,35] developed a theory with rationalization that the hydrodynamic interaction and the excluded volume effect are screened in concentrated solution. The final formulation reads as:

$$n = d(d+2-2d_f)/2(d+2-d_f) \tag{8}$$

Calculated values of d_f from equation (8) are summarized in *Table 2*. Generally, static light scattering on dilute solutions of polymer clusters makes it possible to determine d_f. Unfortunately we could not stop the chemical reaction of this system as required. Similar work on another end-linking system is in progress using dynamic viscoelasticity as well as static and dynamic light scattering.

ACKNOWLEDGEMENTS

One of the authors (NN) is grateful to Professors M. Muthukumar and H. H. Winter for valuable discussions. We thank Kaneka Corporation for supplying the prepolymer samples and catalyst.

REFERENCES

1 Chambon, F. and Winter, H. H. *Polym. Bull.* 1985, **13**, 499
2 Winter, H. H. and Chambon, F. *J. Rheol.* 1986, **30**, 367
3 Chambon, F., Petrovic, Z. S., MacKnight, W. J. and Winter, H. H. *Macromolecules* 1986, **19**, 2146
4 Chambon, F. and Winter, H. H. *J. Rheol.* 1987, **31**, 683
5 Winter, H. H. *Progr. Colloid Polym. Sci.* 1987, **75**, 104
6 Winter, H. H., Morganelli, P. and Chambon, F. *Macromolecules* 1988, **21**, 532
7 Valles, E. M., Carella, J. M., Winter, H. H. and Baumgaertel, M. *Rheol. Acta* 1990, **29**, 535
8 Scanlan, J. C. and Winter, H. H. *Macromolecules* 1991, **24**, 47
9 Izuka, A., Winter, H. H. and Hashmoto, T. *Macromolecules* 1992, **25**, 2422
10 Adam, M., Delsanti, M. and Durand, D. *Macromolecules* 1985, **18**, 2285
11 Durand, D., Delsanti, M., Adam, M. and Luck, J. M. *Europhys. Lett.* 1987, **3**, 297
12 Lairez, D., Adam, M., Emery, J. R. and Durand, D. *Macromolecules* 1992, **25**, 286
13 Martin, J. E., Adolf, D. and Wilcoxon, J. P. *Phys. Rev. Lett.* 1988, **61**, 2620
14 Adolf, D., Martin, J. E. and Wicoxon, J. P. *Macromolecules* 1990, **23**, 527
15 Hodgson, D. F. and Amis, E. J. *Macromolecules* 1990, **23**, 2512
16 Muller, R., Gerard, E., Dugand, P., Rempp, P. and Gnanou, Y. *Macromolecules* 1991, **24**, 1321
17 Antonietti, M., Folsch, K. J., Sillescu, H. and Pakula, T. *Macromolecules* 1989, **22**, 2812
18 Schmidt, M. and Burchard, W. *Macromolecules* 1981, **14**, 370
19 Schosseler, F. and Leibler, L. *J. Phys. Lett.* 1984, **45**, 501
20 Martin, J. E. and Keefer, K. D. *Phys. Rev. A* 1986, **34**, 4988
21 Martin, J. E., Wilcoxon, J. P. and Adolf, D. *Phys. Rev. A* 1987, **36**, 1803
22 Martin, J. E. and Wilcoxon, J. P. *Phys. Rev. Lett.* 1988, **61**, 373
23 Dietler, G., Aubert, C., Cannell, D. S. and Wiltzius, P. *Phys. Rev. Lett.* 1986, **57**, 3117
24 Adam, M., Delsanti, M., Munch, J. P. and Durand, D. *Phys. Rev. Lett.* 1988, **61**, 706
25 Vacher, R., Woignier, T., Pelous, J. and Courtens, E. *Phys. Rev. B* 1988, **37**, 6500
26 Patton, E. V., Wessen, J. A., Rubinstein, M., Wilson, J. C. and Oppenheimer, L. E. *Macromolecules* 1989, **22**, 1946
27 Ferri, F., Frisken, B. J. and Cannell, S. *Phys. Rev. Lett.* 1991, **67**, 3626
28 Stockmayer, W. H. *J. Chem. Phys.* 1943, **11**, 45
29 Flory, P. J. 'Principles of Polymer Chemistry', Cornell University Press, Ithaca, 1953
30 de Gennes, P. G. 'Scaling Concepts in Polymer Physics', Cornell University Press, Ithaca, 1979
31 Stauffer, D. 'Introduction to Percolation Theory', Taylor and Francis, London, 1985
32 Herrmann, H. J., Landau, D. P. and Stauffer, D. *Phys. Rev. Lett.* 1982, **49**, 412
33 Herrmann, H. J., Stauffer, D. and Landau, D. P. *J. Phys. A* 1983, **16**, 1221
34 Muthukumar, M. *J. Chem. Phys.* 1985, **83**, 3161
35 Muthukumar, M. *Macromolecules* 1989, **22**, 4656
36 Muthukumar, M. and Winter, H. H. *Macromolecules* 1986, **19**, 1285
37 Martin, J. E., Adolf, D. and Wilcoxon, J. P. *Phys. Rev. A* 1989, **39**, 1325
38 Hess, W., Vilgis, T. A. and Winter, H. H. *Macromolecules* 1988, **21**, 2536
39 Vilgis, T. A. *Progr. Colloid Polym. Sci.* 1992, **90**, 1
40 Takahashi, M., Takigawa, T., Yokoyama, K. and Masuda, T. to be published
41 Graessley, W. W. and Edwards, S. F. *Polymer* 1981, **22**, 1329